Structural studies of laterally attached liquid crystalline polymers

PLEASE SCROLL DOWN FOR ARTICLE

Structural studies of laterally attached liquid crystalline polymers

by A. S. CHERODIAN, N. J. HUGHES and R. M. RICHARDSON*

School of Chemistry, University of Bristol,
Cantock's Close, Bristol BS8 1TS, England

M. S. K. LEE† and G. W. GRAY‡

School of Chemistry, University of Hull,
Hull HU6 7RX, England

Structural studies of a series of laterally attached side chain liquid crystalline polysiloxanes have been made by X-ray diffraction. All but one exhibit a nematic phase with S_C-like short range ordering. The diffraction has been interpreted in terms of a model in which the mesogenic units form a 'jacket' around the polymer backbone. The backbone conformation has been studied by small angle X-ray scattering from oriented samples of mesomorphic solutions and by infrared dichroism measurements on oriented samples of the polymers. In both cases the results were consistent with the mesogens being oriented parallel to the backbone which is consistent with the 'mesogen jacket' model.

1. Introduction

In recent years, a new class of side chain liquid crystal polymers (SCLCPs) has been synthesized and studied. In these compounds, the side chain mesogenic units are attached laterally through flexible spacers [1–10]. None of these polymers has exhibited smectic mesomorphism. All of them have only a nematic mesophase independent of the nature of the backbone, the length of the flexible spacers, or the length of the terminal group on the mesogenic units. Finkelmann reasoned that attaching the polymer backbone by flexible spacers to a lateral point on the mesogenic units would restrict the rotation of the side chain mesogenic groups about their long axes. He suggested that this would give rise to biaxial mesophases; conoscopic observations were made on an oriented sample of an acrylate system, where the nematic phase was judged to be biaxial [2]. On the basis of the spatial requirements of the long mesogenic groups Zhou et al. [5, 6] speculated that the side chain mesogenic groups are oriented parallel to the polymer backbone forming a jacket around it. A distinct feature of the polyacrylate synthesized by them, was that the mesogenic unit was linked to the polyacrylate backbone by only one methylene unit. They reasoned that, since the side chains are bonded to the backbone at a site close to the centres of the mesogenic groups, the motions of the backbone segments would have only minor effects on the motion of the mesogenic units. Therefore the use of flexible spacers, which in conventional terminally attached SCLCPs is required to decouple the motions of the

---

* Author for correspondence.
† Present address: Manchester Polymer Centre, Department of Chemistry, University of Manchester, Oxford Road, Manchester M13 9PL, England.
‡ Present address: Merck Ltd, West Quay Road, Poole, Dorset BH15 1HX, England.

backbones and the side chain segments, are thought to be of less importance in the case of laterally attached SCLCPs. Recent neutron scattering experiments on a deuterium-labelled polysiloxane sample of this type have given evidence of this 'mesogenic jacketed' structure [12].

Here we report on a systematic structural study of a series of side chain liquid crystalline polysiloxanes synthesized at Hull University [7–10]. The polymers are listed in table 1. Mesogenic units of types A and B are attached laterally to either poly(hydrogenmethylsiloxane)[PHMS] or poly(hydrogenmethyldimethylsiloxane) [P(HM/DM)S] backbones by flexible spacers of 5 or 6 methylene groups, i.e. $n = 5$ or 6. In addition side chain copolymers consisting of mixtures of side chains A and B in varying ratios have been studied. Transition temperatures were obtained by differential scanning calorimetry (DSC) and optical microscopic studies performed at Hull University; data are also listed in table 1. Section 2 reports X-ray diffraction results from these materials. We have found it necessary to complement these results with small angle scattering studies which are reported in §3 and infrared dichroism measurements which are in §4.

2. X-ray diffraction studies

2.1. *Experimental*

Diffraction studies have been made on powder and aligned polymer samples using monochromatic Cu–K$_\alpha$ radiation. Diffraction patterns from each sample were recorded using a linear or a two dimensional position sensitive detector (i.e. an area detector) [13]. The samples were placed in an electrically heated oven which was mounted on the diffractometer and the temperature was regulated by a Eurotherm controller to within $\pm 0.5°$C. The oven was also fitted with Peltier coolers and water cooled blocks in order to achieve temperatures below room temperature. Diffraction patterns were recorded, at selected temperatures, on cooling the samples from the isotropic state. Orientation of the samples was achieved by drawing fibres from the nematic melt of the polymer. This was done using an oven that was designed for drawing fibres when mounted on the diffractometer. In some cases the fibres lasted only a few minutes, which was found to be adequate to obtain a reasonable diffraction pattern using the area detector system [13]. Polymers VII and X were found to be too fluid to draw into fibres. In addition, aligned samples of polymers I and VI, contained in Lindemann tubes, were obtained by cooling from the isotropic state to room temperature, at a rate of $10°$C h^{-1} in an 11 T magnetic field. The samples were then removed from the magnetic field and mounted on the diffractometer.

2.2. *Results and discussion*

Powder samples of each polymer were used to record the variation in the d-spacing of the various peaks on cooling the sample from its isotropic state ($d = \lambda/(2 \sin \theta)$; where 2θ is the scattering angle and λ the X-ray wavelength). The diffraction patterns for all polymers except polymer V (which is discussed in §2.2.5) were found to be similar—a diffuse peak at small angles and two broad diffuse peaks at wide angles. The absence of any Bragg reflections showed that the samples were in the nematic state over the entire temperature range of the mesophase. The nematic–isotropic transitions could not be detected from the diffraction patterns obtained from powder samples.

Diffraction patterns of the oriented samples (fibres or magnetically aligned) were recorded at room temperature in their nematic or glassy states using an area detector.

Downloaded At: 11:08 26 January 2011

Table 1.

A

C₈H₁₇O—⟨benzene⟩—COO—⟨biphenyl⟩—CN
            O(CH₂)ₙ—

B

C₈H₁₇O—⟨benzene⟩—COO—⟨biphenyl⟩—C₅H₁₁
            O(CH₂)ₙ—

Homopolymer (PHMS) backbone

$(CH_3)_3SiO$ —[Si(CH_3)(O)—A]ₓ—[Si(CH_3)(O)—B]ᵧ— Si(CH_3)₃   X+Y = 46 +/-3

	Polymer	$X/X+Y$	$Y/X+Y$	n	T_g	T_{NI}
					Transition temperatures/°C	
Side chain homopolymers	I	1	0	5	29·4	89·8
	II	1	0	6	25·1	82·1
	III	0	1	5	1·2	42·4
	IV	0	1	6	−8·6	41·6
Side chain copolymer	V	0·5	0·5	5	5·7	37·9

Copolymer {P(HM/DM)S} backbone

$(CH_3)_3SiO$ —[Si(CH_3)(O)—A]ₓ—[Si(CH_3)(O)—B]ᵧ—[Si(CH_3)(O)(CH_3)]_z— Si(CH_3)₃   X+Y+Z = 13 +/-2

X+Y : Z = 1 : 1.7

	Polymer	$X/X+Y$	$Y/X+Y$	n	T_g	T_{NI}
					Transition temperatures/°C	
Side chain homopolymers	VI	1	0	5	−12·5	36·6
	VII	0	1	5	−22·0	23·6
Side chain copolymer	VIII	0·6	0·4	5	−13·8	28·5
	IX	0·5	0·5	5	−16·8	23·8
	X	0·4	0·6	5	−16·6	24·9

Because of the alignment procedure, the samples have a uniaxial symmetry around the meridian, i.e. the magnetic field direction or the fibre axis for the fibre samples. The observed diffraction patterns from all the oriented samples were almost identical. Hence we shall first consider the diffraction features that were observed for polymer I and then discuss the subtle differences that were observed for the other polymers.

Figure 1 shows the diffraction pattern from a magnetically aligned sample of polymer I which has a PHMS backbone and a cyano terminal group on the side chain
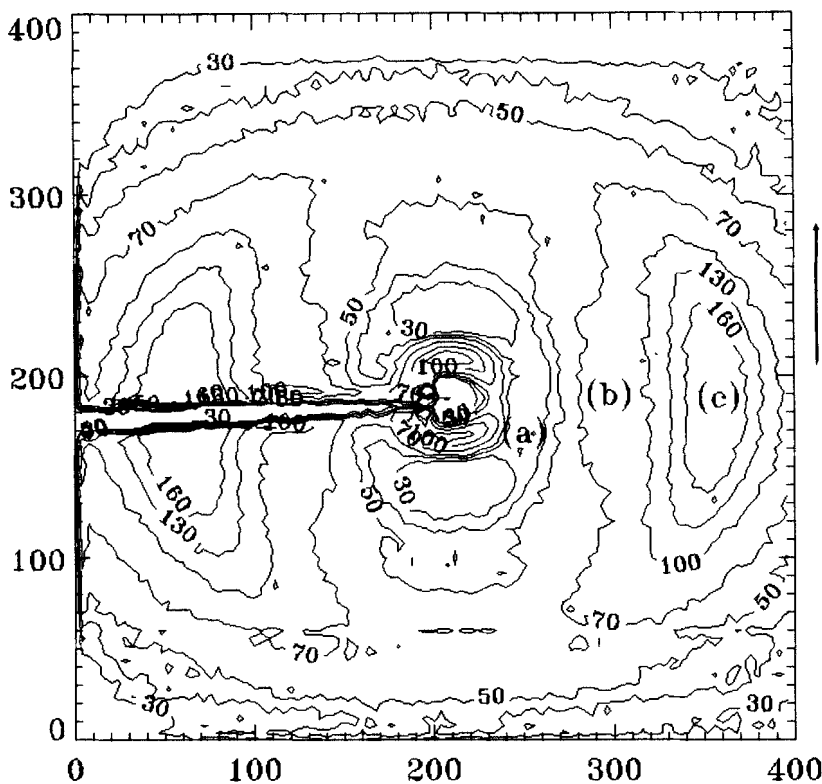
Figure 1.   X-ray diffraction pattern from a magnetic field aligned sample of polymer I at 28°C. Arrow indicates the direction of the magnetic field (*B*).

moiety. The marked anisotropy of the molecular organization is clearly observed by the presence of two diffuse, wide angle crescents (labelled c in figure 1) on the equator. These diffuse arcs of scattering correspond to a repeat distance of about 4·5 Å and are associated with the lateral correlations between the mesogenic units. They are very similar to those observed for low molar mass liquid crystals [14] and correspond to the distance between nearest neighbours. The location of these diffuse maxima implies that the mesogenic groups have a preferred orientation parallel to the fibre axis or the direction of the magnetic field.

In well-aligned samples, four symmetrical diffuse spots are resolved at small angles indicating smectic-like short range ordering of the mesogenic units. These can be clearly seen in figure 7. They are two Freidel pairs (labelled *a* in figure 1) making an angle with the meridian, implying smectic C-like short range ordering. Other workers [11] have also observed similar short range effects in the nematic phase of a laterally attached polysiloxane. Such pronounced smectic C fluctuations are often related to the occurrence of 'skewed cybotactic groups' [15] and have been known to occur in the nematic phases of conventional terminally attached SCLCPs [16] and low molar mass liquid crystals [15, 19]. They are, however, usually associated with nematic phases which transform to a S_C phase at lower temperatures. Since smectic mesomorphism has not been observed in the laterally attached side chain polysiloxanes we have studied, the inference of cybotactic groups is unexpected, particularly since the terminal cyano group tends to favour the formation of nematic or smectic A phases. It therefore

appears that smectic C-like short range ordering is a characteristic of the nematic phase of laterally attached side chain liquid crystal polymers.

From a plot of the intensity (averaged across a narrow strip) as a function of the angle made with the meridian, the tilt angle of the mesogenic groups with respect to the pseudo-layer normal is estimated at $\sim 17°$. Since the d-spacing of the diffuse spots is ~ 27 Å and the length of the side chain mesogenic groups, calculated from CPK models, is ~ 29 Å, there is a negligible overlap of the mesogenic units.

Higher orders of these four diffuse spots are also observed in polymer I. These can be indexed as the 3rd, 5th and 7th order peaks. The presence of so many higher orders of peak resulting from end to end correlation in the nematic phase is unusual and would imply a higher degree of translational ordering along the director direction. The absence of the even order peaks is probably an effect of the form factor of the mesogenic units. The electron density of a mesogenic unit projected onto the director would be expected to have a maximum near the middle of the unit, due to the flexible spacer, and a minimum at either end in the 'gap' between units. The amplitude of the even Fourier components in such a distribution is low, so only the odd ones dominate the form factor, and hence only the odd peaks have appreciable intensity.

It is well known from the study of low molar mass liquid crystalline materials that the presence of a terminal cyano group induces a strong longitudinal dipole in the mesogenic core and this induces the formation of antiparallel pairs of overlapping molecules. As a result of this, in the nematic phase, a damped density wave with a d-spacing considerably greater than the molecular length is observed (typically $\sim 1.4l$ or $l +$ the length of the alkyl tail; where $l =$ length of the molecule) [17–19]. In the smectic A phase however, a partial bilayer structure $(l < d < 2l)$ is induced (the S_{Ad} phase) due to the antiferroelectric organization of the molecules [18–22]. S_{Ad} phases are also common in terminally attached SCLCPs having cyano end groups [23–26], but in these laterally attached SCLCPs, the effect of the backbone has been to suppress the packing involving 'overlapping cores' of the mesogenic units.

The last feature of the diffraction pattern is a pair of diffuse peaks in the equatorial plane (marked b in figure 1). This feature has also been observed by Hardouin et al. [11]. In the polymers studied here, the d-spacing for these peak shifts from 8 Å to 9 Å when the length of the flexible spacers is increased from five to six CH_2 units (see figures 6 and 7) and was found to be 7 Å when the flexible spacer is four CH_2 units long [11]. These observations suggest that these peaks arise from objects separated by the flexible spacer. Another observation is that these peaks are much narrower in the direction parallel to the director than the diffuse arcs (c in figure 1). The extent of the latter is determined by the length of the mesogenic units ($\Delta Q \sim 4\pi/l$), plus some additional smearing into arcs due to imperfect alignment of the mesogenic units with the director. The extra diffuse peaks (marked (b)) are more closely confined to the equator of the diffraction pattern. This suggests that they result from interference from objects which extend further along the director and are more closely aligned parallel to it. The following interpretation of the extra diffuse peaks is therefore proposed:

(i) The siloxane backbones lie predominantly parallel to the director.

(ii) The mesogenic units lie parallel to the backbone with the spacer extended.

(iii) The mesogenic units tend to spiral around the backbone because of packing restrictions.

Each chain will therefore consist of two regions of high electron density, i.e. the central rod of the siloxane backbone and a coaxial sheath of mesogenic units. If we

assume (for simplicity) that equal numbers of electrons contribute to these regions, the scattering expected in the equatorial plane would be in the form:

$$I(Q_\perp) \approx (1 + J_0(Q_\perp))^2$$

where J_0 represents a cylindrical Bessel function and a is the radius from the backbone to the centre of the mesogenic unit. The function $J_0(x)$ has its first maximum $x = 7 \cdot 0$. For the polymer with five methylene units in its spacer, the extra diffuse peaks occur at $Q = 0 \cdot 76 \, \text{Å}^{-1}$, so the above equation implies a radius a of $9 \cdot 2 \, \text{Å}$. This agrees well with the backbone to mesogenic unit distance measured from CPK models and supports our interpretation of the diffuse peaks (*b*).

2.2.1. *Orientation of the backbone*

The wide angle X-ray scattering data show no direct evidence to indicate whether the side chains are oriented parallel or perpendicular to the polymer backbone. The only indication we have is the success of the model proposed above to explain the diffuse peaks, (*b*), which are a feature of laterally attached SCLCPs. Zhou *et al.* [5, 6] have proposed the term 'mesogen jacketed polymer' to describe the laterally attached polyacrylate that they have synthesized. They suggested that the spatial requirements of the long mesogenic units necessitate that the mesogenic units pack parallel to each other as well as to the polymer backbone, forming a 'mesogen jacket' around it. Although the orientation of the mesogenic units in drawn fibres would be consistent with this model, it could be wrong to assume that the backbones would prefer to align along the direction of drawing in drawn figures. X-ray studies on other types of liquid crystal polymers, such as terminally attached SCLCPs and main chain polymers, have shown that the orientation of the mesogenic groups with respect to the fibre axis was influenced by several factors. The phase of the polymer melt from which the fibre is drawn [27, 28], the length of the flexible spacer [25], the nature of the backbone [29], and the molecular weight of the polymer [30] have all been found to have an influence.

We have therefore sought additional techniques to confirm the orientation of the polymer backbone with respect to the mesogenic unit. Hardouin *et al.* [12] were the first to provide evidence for the mesogen jacketed model for the nematic phase of a deuteriated laterally attached polysiloxane by small angle neutron scattering experiments. Unfortunately, suitable deuteriated versions of the materials studied here were not available, so small angle X-ray scattering and infrared dichroism measurements have been used. These are described in §§ 3 and 4.

The mesogen jacketed model is illustrated in figure 2, where the side chain mesogenic units are oriented parallel to the backbone. In the SCLCPs having the PHMS backbone there is a mesogen linked on every silicon atom (i.e. every $2 \cdot 5 \, \text{Å}$) which would cause adjacent mesogens to be displaced along the direction of the long axis of the backbone. We can, therefore, envisage the occurrence of smectic C-like short range order regardless of the nature of the side chain mesogenic groups. The helical organisation of the mesogenic units, driven by packing constraints, naturally results in the S_C-like short range ordering. For such a model the mesogenic units will be constrained to lie at a certain distance from the siloxane backbone by the flexible spacers. This restriction probably explains why an 'overlapping cores' type of short range ordering of the mesogenic units is not observed in the nematic phases of laterally attached polymers. It might also explain why the end to end ordering of the mesogenic units is strong compared to low molar mass nematic materials, resulting in the observation of higher order bands of scattering.
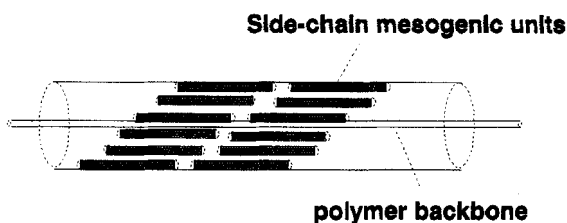
Side-chain mesogenic units

polymer backbone

Figure 2. Illustration of the 'mesogen jacketed' model for laterally attached side chain liquid crystal polymers.

2.2.2. *Effect of the backbone*

The d-spacings for the small angle peaks arising from the end to end correlation of the mesogenic units are shown in figures 3 and 4. The first noticeable difference between the backbones is the temperature dependence of the d-spacing. For polymers having the PHMS backbone, the small angle peaks shift to lower d-spacings with reducing temperature (see figure 3), whereas, for those with the copolymeric P(HM/DM)S backbone, there is very little change in the d-spacings, with a tendency to increase with reducing temperature (see figure 4). For laterally attached polysiloxanes, changing the backbone appears to have no significant effect on the d-spacings. This is in contrast to terminally attached side chain polysiloxanes [24], where the smectic layer spacing in the S_{Ad} phase, was found to be larger in polymers having the copolymeric backbone.

Figure 5 shows the diffraction pattern from the magnetically aligned sample of polymer VI. Qualitatively, the peaks at small angles appear to be more diffuse, but a plot of the intensity (averaged over a narrow strip) as a function of the angle made with the meridian shows that short range S_C ordering still exists. The tilt angle measured from the meridian ($\sim 12°$) is slightly less than that observed for polymer I ($\sim 17°$). It appears that the ordering in the copolymeric backbone materials is similar to, but less pronounced than that in the homopolymeric backbone materials. This is confirmed by the absence of higher orders of the small angle peaks that were observed for polymer I. This difference in the strength of the ordering may result from the different degrees of polymerization or the different packing constraints imposed by the two backbones.

2.2.3. *Effect of the length of the flexible spacer*

The effect of the spacer length is independent of the nature of the end group. Diffraction patterns from fibres drawn from polymers III and IV are shown in figures 6 and 7, respectively. The addition of a methylene unit to the flexible spacer (polymer IV) results in the diffuse spots at small angles tilting further away from the meridian. This is also accompanied by a decrease in measured d-spacings (cf. figure 3), which would suggest that the increase in the decoupling of the mesogenic units from the backbone allows the side chain mesogenic units to have a greater tilt ($\sim 20°$) within the pseudo-layers of the cybotactic groups. The effect of the length of the spacer group on the diffuse peak at 8–9 Å has already been discussed above.

2.2.4. *Effect of terminal end groups (CN or C_5H_{11})*

There are no higher order peaks from the end to end correlation of the mesogenic units for the polymers with the non-polar pentyl end group. From figures 3 and 4, we can see that for both types of backbone, the polymers with the pentyl end group, i.e. polymers III and VII, have a d-spacing slightly smaller than their cyano analogues (polymers I and VI). The difference is less pronounced for the polymers with spacers of 6
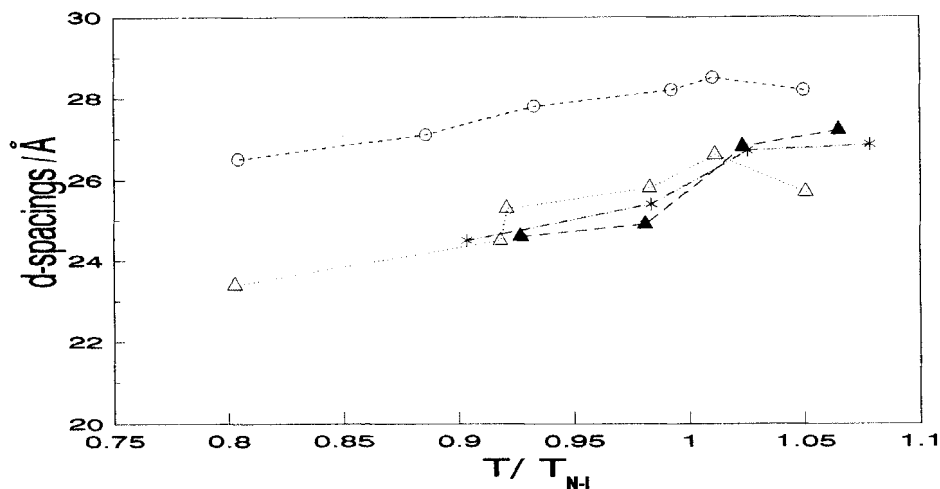
Figure 3.   Variation of the d-spacings of the first order peaks at small angles versus reduced temperature for polymers with the PHMS backbone. ○, I; △, II; ▲, III; *, IV.
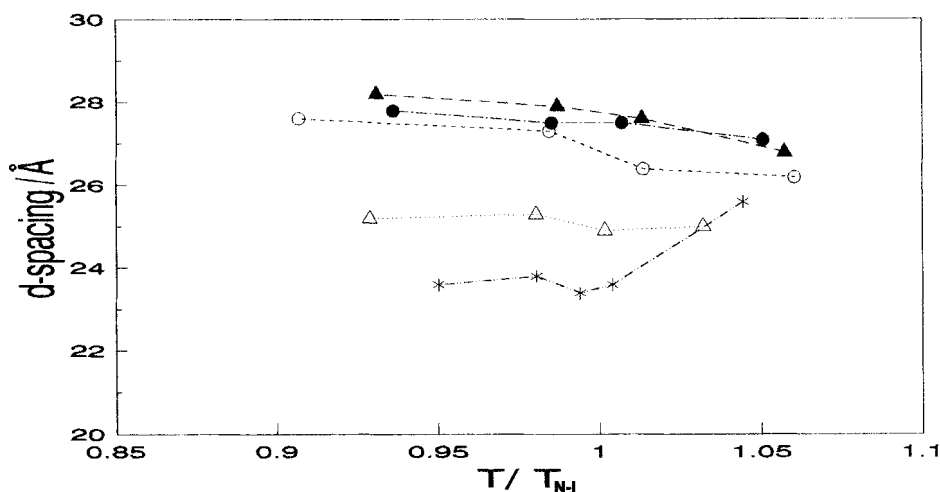

Figure 4.   Variation of d-spacings of peaks at small angles versus reduced temperature for polymers having the copolymeric P(HM/DM)S backbone. ○, VI; △, VII; ▲, VIII; *, IX; ●, X.

methylene units. The measured tilt angles for polymers with the pentyl end group are similar to those observed for their cyano analogues. Since the lengths of the fully extended side chains, measured from CPK models, are about 29 Å and 33 Å for the cyano and pentyl terminated mesogenic units, respectively, the measured d-spacings indicate that the degree of overlap of the mesogenic groups along the director is greater for the polymers with the pentyl end group. The reason that the higher orders of the small angle peak are not observed for the mesogens with the pentyl groups is probably due to the lower electron density variation which results from some overlap of the pentyl end groups.

2.2.5. *Effect of side chain copolymerization*

The primary purpose of synthesising the side chain copolymers, listed in table 1, was to reduce the molecular associations caused by the cyano end groups [10]. This follows from the studies of low molar mass cyanobiphenyls and has important implications in display device applications [31]. It would however be naive to expect a completely random intermixing of the two types of mesogenic unit in the side chain copolymers. This is perhaps reflected in the case of the side chain copolymer V, where the backbone is PHMS. The diffraction pattern (see figure 8) from a drawn fibre of the polymer exhibits an unoriented smectic ring at 34 Å and oriented diffuse nematic peaks at 28 Å. This biphasic behaviour exists throughout the temperature range of the mesophase and was confirmed by diffraction studies on another sample of the same polymer synthesized separately. This is a rare case of smectic layer formation being observed in laterally attached SCLC polysiloxanes. Since neither of the side chain homopolymers, i.e. polymers I and III, exhibit any smectic mesomorphism and in the absence of specimens with different ratios of the two side chains, we can only speculate that the smectic characteristic results from some interaction between the two types of mesogenic unit.
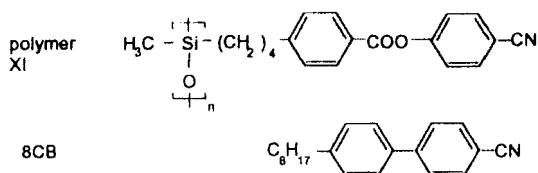
From their *d*-spacings (see figure 4), the backbone/side chain copolymers VIII, IX and X do not show any significant trend when compared to polymers VI and VII. In polymer IX the short range smectic C-like fluctuations still exist, but are substantially reduced. Figure 9 shows the fibre pattern of polymer VII where at small angles only two peaks are observed. A scan of the scattered intensity as a function of the angle made with the meridian suggests enhanced order characteristic of the S_A phase.

3. Small angle X-ray scattering from liquid crystal polymer solutions

The study of conventional polymers in solutions by scattering has proven to be a useful technique. Characteristics of the polymers in solution, such as molar mass, radius of gyration and the second virial coefficient, can be derived from the initial part of the small angle scattering curve without any assumptions as to the specific features of the polymer chain. The classical approach to study the conformation of the polymer chains in liquid crystal polymers is by small angle neutron scattering. This requires the preparation of selectively deuteriated specimens which were not available for this work. Small angle X-ray scattering (SAXS) experiments on solutions of SCLCPs in mesomorphic solvents provide an alternative means of studying the backbone conformation [32–34]. It can only be used on solutions rather than pure liquid crystal polymers and it is limited by lack of contrast between the polymer and the solvent. However, we have used it here to obtain a qualitative indication of the orientation of the polymer backbone with respect to the director.

3.1. *Experimental*

5 and 10 per cent solutions (by weight) of polymer I in 4-cyano-4'-*n*-octylbiphenyl (8CB), a low molar mass liquid crystal, were prepared. As a control similar concentrations of a terminally attached SCLCP (XI) were also studied.
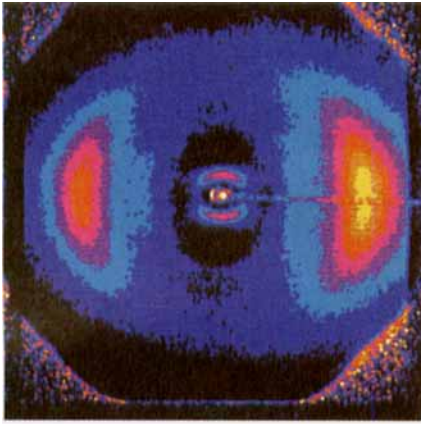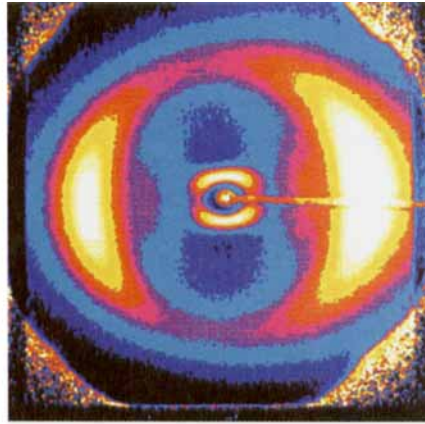
A. S. Cherodian *et al.*
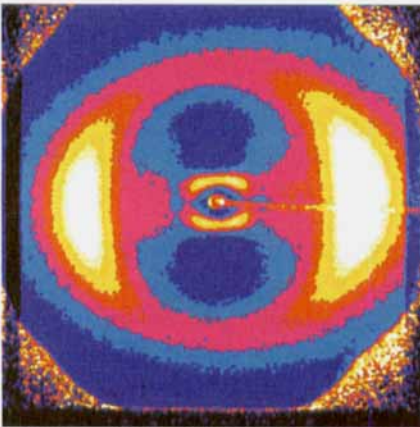

Figure 5.

Figure 6.

Figure 7.

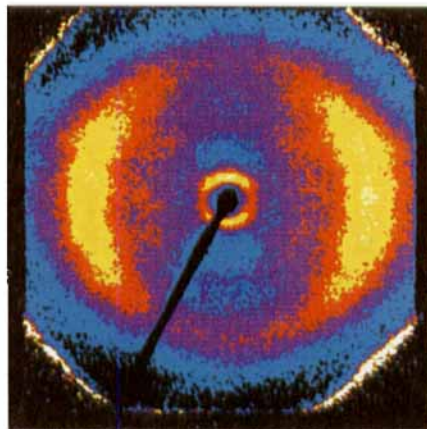Figure 8.

Figure 9.

Table 2. Transition temperatures (°C) by optical microscopy.

Sample	S$_A$—N	N–I or biphasic	Biphasic–I
8CB	29·9	36·5	—
5% Polymer I	31·0	39·8	—
10% Polymer I	28·9	39·2	—
Polymer XI	25·2	136·3	—
5% Polymer XI	31·7	38·8	63·5
10% Polymer XI	32·7	38·5	58·7

Optical microscopy was used to study miscibility of the polymers in 8CB and to obtain the transition temperatures for the solutions. All solutions exhibited a smectic A phase below the nematic phase, following the phase sequence of 8CB. Phase transitions obtained from microscopic studies are listed in table 2. For both the 5 per cent and 10 per cent solutions of polymer I, the textures were found to be different from that observed for the pure polymer or that for 8CB.

The transitions for polymer I were well defined and no biphasic behaviour was observed. From this we deduce that the polymer is miscible in the low molar mass liquid crystal. It was noted that the transition observed for the 5 per cent solution of polymer I was slightly higher than that observed for the 10 per cent solution. In the case of the solutions of the terminally attached SCLCP XI, the transitions were not well-defined and therefore only the approximate temperatures are given. A large biphasic region was observed between the isotropic state and the nematic phase. On cooling down to the mesophase region, domains rich with the polymer were observed in both the nematic and smectic A phases. This implies that the polymer is not completely miscible in the low molar mass solvent. The electron density contrast between the backbone and the solvent was weak and so the small angle scattering was correspondingly weak. Only the 10 per cent solution of polymer I was analysed in detail although the more dilute solution gave qualitatively similar results. Although the validity of these experiments requires the use of homogeneous polymer solutions, the result from the terminally attached polymer solutions are included here as a qualitative comparison of the chain conformation in the terminally attached polymer with that of the laterally attached SCLCP.

Figure 5.   X-ray diffraction pattern from a magnetic field aligned sample of Polymer VI at 28°C. Arrow indicates the direction of the magnetic field (*B*).

Figure 6.   X-ray diffraction pattern from a drawn fibre sample of polymer III at 28°C. Arrow indicates the direction of draw.

Figure 7.   X-ray diffraction pattern from a drawn fibre sample of polymer IV at 28°C. Arrow indicates the direction of draw.

Figure 8.   X-ray diffraction pattern from a drawn fibre sample of polymer V (28°C) showing oriented diffuse peaks and a smectic layer ring. Arrow indicates the direction of draw.

Figure 9.   X-ray diffraction pattern from a drawn fibre sample of polymer VIII (28°C). Arrow indicates the direction of draw.
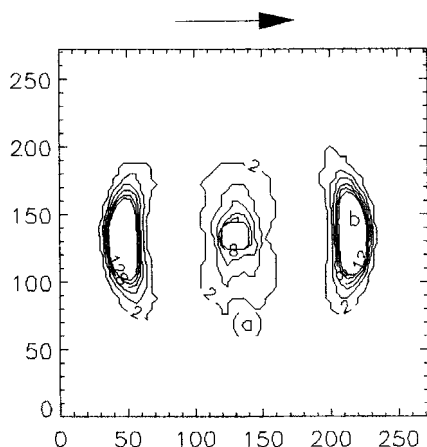
Figure 10.   Contour plot of small angle X-ray scattering from a 10 per cent solution of polymer I in the nematic state. Arrow indicates the direction of the magnetic field (B).

The samples were contained in flat cells and placed in an oven fitted with permanent magnets. The temperature was regulated to $\pm 0.5°C$ using a Eurotherm controller. Orientation of the sample was obtained by slow cooling from the isotropic state in a 0·25 T magnetic field. Measurements were carried out using the small angle scattering apparatus [35] at Bristol. A monochromatic Cu–K_α radiation was used for the experiments, which provided a scattering vector range $0.01\,\text{Å}^{-1} < Q < 0.45\,\text{Å}^{-1}$. Exposure times of 10 h were required and scattering patterns were recorded at selected temperatures in the isotropic state, nematic and S_A phases.

3.2. *Determination of radii of gyration*

Figure 10 shows the small angle scattering from a 10 per cent solution of polymer I in the nematic phase. In the isotropic state the scattering at low Q is isotropic. On cooling to the nematic phase two diffuse peaks are observed ($Q \sim 0.19\,\text{Å}$) along the meridian. These peaks arise principally from the end to end correlation between the mesogenic units and indicate that the mesogenic units are aligned preferentially parallel to the magnetic field. These peaks condense into Bragg spots in the S_A phase. At smaller angles ($Q < 0.1\,\text{Å}^{-1}$) there is an anisotropic distribution of the scattered intensity. Therefore, the measured intensities in pixels at equal distances from the beam centre were averaged to improve the statistics. Equal sectors parallel and perpendicular to the meridian (direction of the magnetic field) were grouped so that the radial distributions of the scattered intensity in the two directions were obtained. The distributions of the scattering from the polymer chains were obtained by subtracting the background distribution of scattered intensities produced by an oriented sample of pure 8CB and normalised using the isotropic scattering from a ^{55}Fe source.

Due to the limited miscibility of polymer XI, the anisotropy of the scattering at lower Q was rather poor. The best results were obtained from the 5 per cent concentration and are used here to compare results from the laterally attached SCLCP. Figure 11 shows the scattering pattern from the 5 per cent solution of polymer XI. Since we were only able to measure SAXS from one concentration with reasonable signal : background ratio, it was not feasible to extrapolate to a concentration of zero.
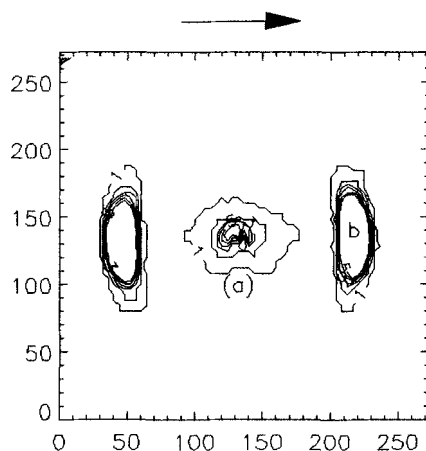
Figure 11.   Contour plot of small angle X-ray scattering from a 5 per cent solution of polymer XI in the nematic state. Arrow indicates the direction of the magnetic field (*B*).

Table 3.   Radius of gyration values parallel ($R_\parallel$) and perpendicular ($R_\perp$) to the director.

	Mesophase (temperature)	$R_\parallel/\text{Å}$	$R_\perp/\text{Å}$	Anisotropy ratio ($R_\parallel/R_\perp$)
10% Polymer I	Nematic (33°C)	42 ± 4	26 ± 3	1·6
	S_A (27°C)	53 ± 6	33 ± 3	1·6
5% Polymer XI	Nematic (33°C)	24 ± 2	27 ± 3	0·9
	S_A(27°C)	24 ± 2	30 ± 3	0·8

We have therefore assumed that the concentration dependence is not dramatic and have analysed the solutions using the Guinier approximation

$$I(Q) \approx I(0)\exp(-Q^2 R_x^2/3),$$

where $R_x = R_\parallel$ or $R_\perp$. This is valid in the region $QR_x < 1$. $R_\parallel$ or $R_\perp$ is the root mean square distance from the centres of mass of the polymer segments projected onto an axis parallel or perpendicular to the director. They are related to the familiar radius of gyration, R_G, of a polymer molecule

$$R_\parallel^2 + 2R_\perp^2 = 3R_G^2.$$

These second moments have been determined from the slope of 'Guinier' plots of log (I) versus Q^2. Values of $R_\parallel$ and $R_\perp$ were obtained for the nematic and smectic phases and are given in table 3. For polymer *I*, $R_\parallel > R_\perp$ which corresponds to a prolate (rod-like) shape of the backbone elongated in the direction of the magnetic field. This is consistent with the mesogen jacketed model. In the nematic phase, the anisotropy ratio, $R_\parallel/R_\perp \sim 2$, is low. This indicates that the siloxane backbone is not very well confined along the director. There is no significant change in conformation of the chains in the smectic A phase. Although these results cannot be transposed directly to the neat liquid crystal polymer, they do suggest that the backbone has a tendency to lie parallel to the mesogenic units, at least in the solutions, but the degree of alignment is not very high. In contrast, $R_\parallel < R_\perp$ for the 5 per cent solution of polymer XI, and hence an oblate conformation of the backbone is implied.

4. Infrared dichroism measurements

A sample of polymer VI was prepared by filling an approximately $10\,\mu$m gap between two KRS5 plates and aligned by cooling from the isotropic state to room temperature in a 7T magnetic field. Polarized infrared absorption spectra were recorded with the plane of polarization at 15° intervals between parallel and perpendicular to the alignment direction. After some analysis two bands were selected from the spectra for more quantitative treatment.

(i)   The 2226 cm^{-1} band from the C≡N stretch was identified as giving a good indication of the orientation of the mesogenic unit.

(ii) The 762 cm^{-1} band was identified as resulting from Si–CH$_3$ stretch where the Si was also attached to a mesogenic unit. It was therefore expected to have its transition dipole perpendicular to the backbone and at an angle ∼108° to the mesogenic unit.

The areas of the peaks in the absorbance have been plotted against $\cos^2 \theta$, where θ is the angle between the alignment direction and the plane of polarization, and straight line fits are shown in figure 12. The conventional dichroic ratio (R = absorbance$_{\parallel}$/absorbance$_{\perp}$) can be determined from the intercepts and the slopes of the fits.

The dichroic ratio may be converted into an orientational order parameter for these transitional dipoles using the formula

$$S = \frac{R-1}{R+2}.$$

The resultant order parameters are shown in table 4. They confirm that the alignment of the mesogenic units is parallel to the aligning field. The degree of alignment is rather low, possibly because of insufficiently slow cooling in the magnetic field. However, the Si–CH$_3$ bonds do tend to be perpendicular to the C≡N bonds which suggests that the backbone must lie parallel to the mesogenic units and provides additional confirmation of the mesogen jacketed model for these materials.
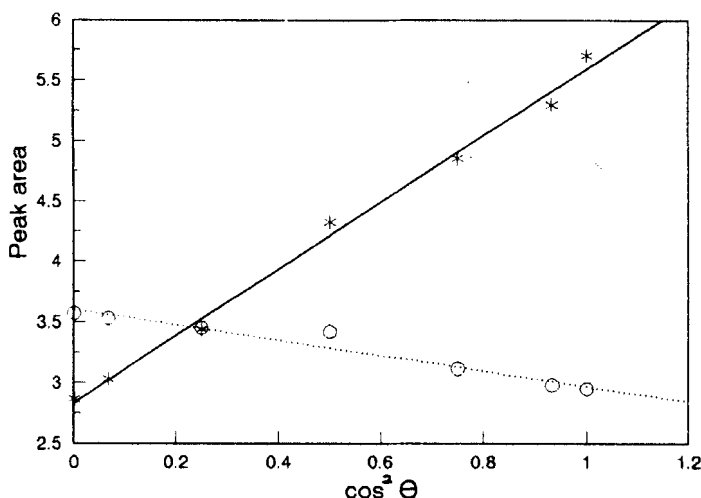

Figure 12.   Infrared dichroism results showing absorbance peak areas versus $\cos^2 \theta$, where θ is the angle between the polarization and the alignment direction. *, 2226 cm^{-1}; ○, 762 cm^{-1}.

Table 4. Dichroic ratio and order parameter for the $2226\,\text{cm}^{-1}$ and $762\,\text{cm}^{-1}$ absorption bands.

	Mesogenic unit ($2226\,\text{cm}^{-1}$)	Backbone ($762\,\text{cm}^{-1}$)
R	1·96	0·82
S	0·24	−0·06

5. Conclusion

We have shown that in the nematic phase formed by these laterally attached side chain liquid crystal polymers, both the side chain mesogenic unit and the backbone lie parallel to the director.

An analysis of the diffuse peaks in the diffraction pattern has suggested that there is a tendency for the mesogenic units to spiral around the backbone as suggested by the mesogen jacketed model [5, 6] shown in figure 2. The orientation of the backbone with respect to the mesogenic groups has been confirmed by small angle scattering measurements from mesomorphic solutions and by infrared dichroism measurements. The constraints imposed on the mesogenic unit have apparently suppressed the tendency for the cyano terminated materials to adopt the 'overlapping core' packing so ubiquitous in similar low molecular weight compounds.

References

[1] HESSEL, F., and FINKELMANN, H., 1985, *Polym. Bull.*, **14**, 375.
[2] HESSEL, F., and FINKELMANN, H., 1985, *Polym. Bull.*, **15**, 349.
[3] HESSEL, F., HERR, R. P., and FINKELMANN, H., 1987, *Makromolek. Chem.*, **188**, 1597.
[4] KELLER, P., HARDOUIN, F., MAUZAC, M., and ACHARD, M. F., 1988, *Molec. Crystals liq. Crystals*, **155**, 171.
[5] ZHOU, Q. F., LI, H. M., and FENG, X. D., 1987, *Macromolecules*, **20**, 233.
[6] ZHOU, Q. F., LI, H. M., and FENG, X. D., 1988, *Molec. Crystals liq. Crystals*, **155**, 73.
[7] GRAY, G. W., HILL, J. S., and LACEY, D., *Molec. Crystals liq. Crystals*, **197**, 43.
[8] LEE, M. S. K., GRAY, G. W., LACEY, D., and TOYNE, K. J., 1989, *Makromolek. Chem rap. Commun.*, **10**, 325.
[9] LEE, M. S. K., GRAY, G. W., LACEY, D., and TOYNE, K. J., 1990, *Makromolek. Chem. rap. Commun.*, **11**, 109.
[10] LEE, M. S. K., 1991, Ph.D. Thesis, University of Hull, Hull, England.
[11] HARDOUIN, F., MERY, S., ACHARD, M. F., MAUZAC, M., DAVIDSON, P., and KELLER, P., 1990, *Liq. Crystals*, **8**, 565.
[12] HARDOUIN, F., MERY, S., ACHARD, M. F., NOIREZ, L., and KELLER, P., 1991, *J. Phys. II*, **1**, 511.
[13] BATEMAN, J. E., CONNOLLY, J. F., STEPHENSON, R., FLESHER, A. C., BRYANT, C. J., LINCOLN, A. D., TUCKER, P. A., and SWANTON, S. W., 1987, *Nucl. Instrum. Meth. Phys. Res.* A, **259**, 506.
[14] GRAY, G. W., and WINSOR, P. A., 1974, *Liquid Crystals and Plastic Crystals*, Vol. 2 (Ellis Horwood), p. 62.
[15] DE VRIES, A., 1970, *Molec. Crystals liq. Crystals*, **10**, 219.
[16] DECOBERT, G., SOYER, F., DUBOIS, J. C., and DAVIDSON, P., 1985, *Polym. Bull.*, **14**, 549.
[17] LEADBETTER, A. J., RICHARDSON, R. M., and COLLINGS, C. N., 1975, *J. Phys., Paris*, **36**, Cl-17.

[18] LEADBETTER, A. J., FROST, J. C., GAUGHAN, J. P., GRAY, G. W., and MOSLEY, A., 1979, *J. Phys., Paris*, **40**, 375.

[19] BROWNSEY, G. J., and LEADBETTER, A. J., 1980, *Phys. Rev. Lett.*, **44**, 1608.

[20] HARDOUIN, F., LEVELUT, A. M., BENATTAR, J. J., and SIGAUD., G., 1980, *Solid St. Commun.*, **33**, 337.

[21] HARDOUIN, F., and LEVELUT, A. M., 1980, *J. Phys., Paris*, **41**, 41.

[22] LEVELUT, A. M., TARENTO, R. J., HARDOUIN, F., ACHARD, M. F., and SIGAUD, G., 1981, *Phys. Rev. A*, **24**, 163.

[23] RICHARDSON, R. M., and HERRING, N. J., 1985, *Molec. crystals liq. Crystals*, **123**, 143.

[24] SUTHERLAND, H. H., ALI-ADIB, Z., GASGOUS, B., and NESTOR, G., 1988, *Molec. Crystals liq. Crystals*, **155**, 327.

[25] DAVIDSON, P., and STRZELECKI, L., 1988, *Liq. Crystals*, **3**, 1583.

[26] DAVIDSON, P., and LEVELUT, A. M., 1992, *Liq. Crystals*, **11**, 469.

[27] FREIDZON, Y. A., TALROZE, R. V., BOIKO, N. I., KOSTROMIN, S. G., SHIBAEV, V. P., and PLATÉ, N. A., 1988, *Liq. Crystals*, **3**, 127.

[28] ZENTEL, R., and STROBL, G. R., 1984, *Makromolek. Chem.*, **185**, 2669.

[29] ZENTEL, R., and BENALIA, M., 1987, *Makromolek. Chem.*, **188**, 665.

[30] ZENTEL, R., SCHMIDT, G. F., MEYER, J., and BENALIA, M., 1987, *Liq. Crystals*, **2**, 651.

[31] BRADSHAW, M. J., and RAYNES, E. P., 1983, *Molec. Crystals liq. Crystals*, **91**, 145.

[32] MATTOUSSI, H., and OBER, R., 1990, *Macromolecules*, **23**, 1809.

[33] MATTOUSSI, H., 1990, *Molec. Crystals liq. Crystals*, **178**, 65.

[34] MATTOUSSI, H., 1989, Ph.D. Thesis, Paris VI.

[35] SWANTON, S., 1989, Ph.D. Thesis, University of Bristol, Bristol, England.